

Detectability of the trend in precipitation characteristics over China from 1961 to 2017

Wei Li^{1*}, Yang Chen^{2,3}

1. Key Laboratory of Meteorological Disaster of Ministry of Education, Joint International Research Laboratory of Climate and Environment Change, Collaborative Innovation Center on Forecast and Evaluation of Meteorological Disaster, Nanjing University of Information Science and Technology, Nanjing, China
2. State Key Laboratory of Severe Weather, Chinese Academy of Meteorological Sciences, Beijing, China
3. Technical Support Unit, Working Group-I, IPCC, Université Paris Saclay, Paris, France

* Corresponding Author: Wei Li, Key Laboratory of Meteorological Disaster of Ministry of Education, Joint International Research Laboratory of Climate and Environment Change, Collaborative Innovation Center on Forecast and Evaluation of Meteorological Disaster, Nanjing University of Information Science and Technology, Nanjing, 210044, China

E-mail: weili@nuist.edu.cn

This article has been accepted for publication and undergone full peer review but has not been through the copyediting, typesetting, pagination and proofreading process which may lead to differences between this version and the Version of Record. Please cite this article as doi: 10.1002/joc.6826

Abstract

The detection and attribution of precipitation changes are fundamental for adaptation and mitigation planning. Based on high-quality observations, we determined the detectability of the trends of multiple precipitation characteristics across China using a field significance test. Furthermore, the timing at which spatially-aggregated changes become significant and do not reflect random internal variability was also estimated. The results show that the significant increases in the annual total precipitation (PRCPTOT) and simple precipitation intensity (SDII) and significant decrease in the wet days (WD) are detectable from 1961 to 2017. Namely, the percentage of stations showing these significant trends exceeds that expected by chance. The time of the trend emergence from the mimicked range of internal variability is around 2000 for SDII and WD, while the PRCPTOT trend can only be detected for recent years. The analysis on precipitation of various intensity levels unearths that the significant increases in the amount and frequency of extreme heavy precipitation emerged around 2014, while a significant decreasing trend in light

precipitation might be detected as early as 2000. Global warming is expected to affect the detection of precipitation trends because the timing at which global warming signal in trend of precipitation emerges is consistent with the time at which the trends become significant. In general, significant changes in the PRCPTOT, SDII, and WD occur more frequently in winter than in summer.

Keywords: Trend detection, Time of emergence, Precipitation in monsoon region

1. Introduction

Precipitation characteristics in terms of the amount, frequency and intensity have changed due to human-induced global warming (Karl and Knight 1998; Sun et al., 2007; Liu et al., 2009; Ma et al., 2015a). In particular, light and heavy precipitation, which are closely related to drought and flood risks, respectively, are likely more sensitive to global warming than the mean precipitation (Trenberth et al. 2003; Westra et al., 2013). Thus, the detection of long-term trends of different precipitation characteristics is of particular scientific interest.

Increasing air temperature moisten the atmosphere and therefore alters the hydrological cycle and precipitation patten. In general, the

global mean precipitation will increase at a rate of 1%~3% per 1 °C increase in the temperature (IPCC, 2013; Held and Soden 2006; Sun et al., 2007), largely constrained by the planetary energy balance (Allen and Ingram 2002; Pendergrass and Hartmann 2014). The intensification of extreme precipitation roughly follows the Clausius–Clapeyron rate of—6%~7% per 1 °C increase in the temperature (Dai et al., 2006; Zhao et al., 2012), that is, approximately the same rate as that of the moistening of the atmosphere due to warming (Trenberth et al. 2003). The results of previous studies demonstrated that the past increase in the amount and frequency of precipitation can already be detected on a continental-to-global scale. For example, Zhang et al. (2007) reported an increasing trend at high latitudes and a decreasing trend at subtropical latitudes resulting in a small increase in the global mean precipitation. The increase in extreme precipitation can be more robustly detected than that of the mean precipitation (Zhang et al., 2013). Westra et al. (2012) found that nearly two-thirds of the global weather stations recorded an increase in the annual maximum precipitation from 1990 to 2009, which exhibited a distinct meridional heterogeneity. Donat et al. (2013) also showed that significant increasing trends in extreme precipitation

occurred more frequently than decreasing trends during the 1951-2010 period.

Because of the greater influence of the internal variability on the precipitation at smaller spatial scales, the detection of precipitation changes at a regional scale is more challenging. From an application perspective, it is important to consider countries as a whole to develop a national-level climate policy. A large body of literature is available on precipitation trend estimation for China. A widely used approach is to estimate the trend from daily weather station data aggregated using the area-weighted average (Sun et al., 2014; Yin et al., 2017). For example, Zhai et al. (2005) used data from 750 stations and reported that the significant trends of total and extreme precipitation show large diversity between different regions from 1951 to 2000, resulting in a small change in the trend for the country as a whole. An overall forced signal of the annual maximum precipitation cannot be observed in the observational record up to 2012 (Li et al., 2018). Yin et al. (2018) used updated data from 2400 stations for the period 1961–2017 and found that the maximum one-day precipitation (Rx1day) and very wet days (R95p) averaged over China show increasing trends ($P < 0.01$). Similar results

were obtained in other studies based on gridded daily precipitation recorded at stations (Zhou et al., 2016). However, different gridded datasets show large uncertainties in the national trend estimation for Rx1day, in terms of the magnitude and significance (Yin et al., 2015). The gridded product may contain bias and be potentially misleading because the daily precipitation exhibits a fractal scaling (Lovejoy et al., 2008; Maskey et al., 2016). Therefore, a more robust statistical method should be established to better address the detectability of the trends of the precipitation characteristics at the national scale. This will be an important addition to the detection of the precipitation trend over China.

In this study, we used an intuitive but effective technique to test whether we can clearly detect the overall precipitation trend for China. In addition, the timing at which the trends become significant, that is, distinguishable from random variability, was estimated. The effect of global warming reflecting anthropogenic climate change on the detectability of the trends is also discussed. The findings from this study will not only deepen our understanding of the trends of the precipitation characteristics and effect of anthropogenic global warming on the trend detection over China but also provide important unified background

information for future attribution and projection research.

The remainder of this paper is structured as follows. The data and methodology are described in Section 2. The results of the study are presented in Section 3. Concluding remarks are presented in Section 4.

2. Data and method

2.1 Datasets

This study is based on the analysis of daily precipitation data collected by the China Meteorological Administration at 726 meteorological stations in China from 1961 to 2017 (available online at <http://data.cma.cn/data/cdcdetail/dataCode/A.0029.0001.html>). The dataset has undergone rigorous quality control procedures by the National Meteorological Information Center (Cao et al., 2016); several studies have pointed out that this dataset is relatively homogeneous (Ma et al., 2015b). The stations were retained when the record did not show any missing values in any year during this period, leading to a total of 603 stations in this study. In this study, days with daily precipitation equal to or greater than 1mm were treated as precipitation events. We used the total precipitation (PRCPTOT), wet days (WD), and simple precipitation

intensity (SDII) to represent the magnitude (amount), frequency and intensity of precipitation, respectively. In addition, a percentile-based threshold was applied to divide the precipitation into four categories: light, moderate, heavy, and extreme heavy precipitation. The definitions of the precipitation indices used in this study are listed in Table 1.

2.2 Statistical Methods

The nonparametric Sen's slope method was used to estimate the linear trends of the indices and the nonparametric Mann–Kendall (MK) test was used to assess the statistical significance of the linear trends. This type of method has the advantage of not requiring any distribution form for the indices and has been applied frequently in analyzing indices (Zhang et al., 2004; Alexander and Arblaster, 2009). However, both Sen's slope estimator and the MK test assume that the target data are serially independent. If the time series contains a positive AR (1), the test rejects the null hypothesis more often than specified by the significance level and thus the testing result is unreliable. Considering that serial correlation occurs often in a time series, we adopted the modified approach proposed by Zhang et al. (2000) to properly estimate the serial correlation of a time series and eliminate it from the Sen's slope

estimator and MK test. For the detailed method, please refer to Wang and Swail (2001).

We used a field significance test to examine whether a significant trend can be detected for the country as a whole. In statistics, when a significance test is conducted at the 5% level, 5% of the sites are expected to show a statistical significance even if there is no significant trend. In addition, because the number of sites tested is limited and there are potential correlations among the sites, the percentage of sites showing a statistical significance could be larger than the 5% nominal level if the region does not show a significant trend. To determine whether a temporal trend can be observed, we considered a change in precipitation indices detectable if the percentage of the sites showing significant changes is larger than what is expected by pure chance. Specifically, we constructed a matrix M with stations as column (S) and time series as rows (T). The bootstrap samples were obtained by permuted T 1000 times to form random matrixes M_1^*, \dots, M_{1000}^* . For each resampling matrix, the same sequence of years was used for all stations to ensure that the temporal sequence is removed while retaining spatial dependence. The percentage of stations with a significant increasing trend can be obtained

Accepted Article

for each random matrix and the original non-permuted dataset. If the percentage of stations with a significant increasing trend of the initial matrix was outside 95% of the random distribution (critical value) derived from bootstrap samples, it was regarded as field significant at the 5% significance level. This concept of field significance has been widely used in different regions worldwide (Kiktev et al., 2003; Alexander et al., 2006; Westra et al., 2013; Li et al., 2018).

3. Results

3.1 Detection of precipitation characteristics

Figure 1 shows the trends of the PRCPTOT, WD, and SDII over China from 1961 to 2017 as well as the field significance test results. The percentage of stations showing an increase trend in the PRCPTOT (58.4%) is slightly larger than that showing a decrease (41.6%). Regions with an increasing trend are located mainly in southeastern and western China and regions with decreasing trends are in southeastern to northeastern China. Significant increases occurred on the eastern coast of southeastern China and in northwestern China. Several stations in southwestern China observed a significant decreasing trend. Significant increasing and decreasing trends were observed at 9.5% and 1.7% of the stations,

Accepted Article

respectively. To test whether the percentage of stations with a significant trend is statistically different from the null hypothesis that is expected by random chance, the distribution of the percentage under null hypothesis conditions was generated as a measure of what would be possible by chance. The observed percentage of stations showing a significant positive trend is clearly outside the 95% probability based on 1000 bootstrap realizations, which implies that a clear increase in the PRCPTOT can be detected across China based on the current observational record. However, the observed decreasing trend of the PRCPTOT cannot be detected

A decrease in the WD prevails over almost all of eastern China; southwestern China shows a significant decreasing trend. A significant decrease in the WD can be detected because the percentage of stations with a significant decrease (11.3%) is larger than the critical value (6.2%) deduced from the random distribution. Regions with a significant increase in the WD are mainly located over northwestern China. In total, 7.5% of stations show a significant increasing trend, which is slightly outside the 95% probability distribution.

The SDII increased at 76% of stations, with significant trends at 16.2%

of the stations. Stations with positive trends are mainly located in southeastern China, whereas stations with negative trends are mainly found in North China. Stations with a significant increasing trend occur outside of the random distribution based on bootstrap resampling. This means that intensified daily precipitation can be significantly detected when considering the country as a whole.

We further analyzed the time at which the trend significance emerges by applying the same calculation as that used for the three-year periods before 2011 (1961–1991, 1961–1993, ..., until 1961–2011) and one-year periods after 2011 (1961–2011, 1961–2012, ..., until 1961–2017). We calculated two values for each period. The first value, S , is the percentage of stations showing a significant increasing or decreasing trend. The second value, C (critical value), is a reference value that allows us to reject or accept the null hypothesis of occurrence by pure chance, corresponding to the 95% probability of the distribution constructed with the bootstrap resampling technique. When S was larger than C , we rejected the null hypothesis and adopted the alternative hypothesis that a significant trend could be detected. We also defined the time at which the trend becomes significant when S is first larger than the range of C across

all periods and remains larger over all subsequent periods.

Figure 2 shows the S and C value series for PRCPTOT, SDII, and WD. Because C depends on the number of stations and spatial correlation, C is almost constant for all three indices. For PRCPTOT, the S corresponding to a significant increase could not be detected until recently (~ 2016), while the significant decrease overlaps with the range of C (gray shaded) in all periods. For WD, the percentage of stations with a significant increase shows a slight increasing trend over time, but a significant increase trend does not emerge. However, the percentage of stations with a significant decrease sharply increased from nearly 3% during 1961–1991 to nearly 10% during 1961–2017. The trend became significant before 2000 and remained above the range of C in subsequent periods. The percentage of stations showing a significant increasing trend for SDII is nearly 3% from 1961 to 1991; this value sharply increased to more than 16% from 1961 to 2017. A significant increase trend could be robustly detected before 2010.

We also investigated the relationship between the trend in the precipitation characteristics and global warming, which allowed us to estimate the time of emergence of the forced signal in the precipitation

trend. The detailed methods are described in Text S1. The spatial patterns of the relationships between the precipitation characteristics and global warming (Fig. S1) are almost the same as those in Fig. 1, except that more stations exhibit significant relationships with global warming. The time of emergence of the forced signal in the precipitation trend (Fig. S2) is almost the same as that in Fig. 2. A forced signal can be detected in the increasing trends for PRCPTOT and SDII and decreasing trend for WD. The forced signal can be detected earlier for WD and SDII than for PRCPTOT.

3.2 Detection of the four precipitation categories

Figure 3 shows the trend pattern for the four different precipitation categories. The trends for the light precipitation total (LPT) and light precipitation days (LPD) show similar patterns, with a significant decrease over eastern China and significant increase over northwestern China. An overall significant decrease trend can be clearly detected for the two indices because the percentage of stations showing a significant decrease trend is 12.6% for LPT and 14.3% for LPD. These two values are much larger than the 95% random probability obtained by resampling (Fig. 4). However, a significant increase trend in the light precipitation

cannot be detected because the percentage of stations with a significant increase are overlapped by the pure chance.

The trends in the magnitude and frequency of moderate precipitation show patterns that are almost identical with the trend in the light precipitation, but more stations show significant positive trends in the moderate precipitation total (MPT; 5%) and moderate precipitation days (MPD; 4.3%) compared with LPT (3.6%) and LPD (3.5%). However, the fraction falls below the field significance level. Approximately 11% and 13% of stations show a statistically significant decrease trend for MPT and MPD, respectively, which is much larger than the 95% quantile of the random distribution (Fig. 4).

Significant increases can be observed over southeastern China with respect to the magnitude and frequency of heavy precipitation, which increases the percentage of stations showing a significant positive trend. The percentage of stations with a significant increasing trend, that is, 7.5% for heavy precipitation total (HPT) and 7.0% for heavy precipitation days (HPD), is outside the 95% probability based on 1000 bootstrap realizations, which implies that significant increasing trends in the HPT and HPD can be detected. However, the number of stations with a

Accepted Article

significant negative trend is relatively small, that is, only 1.8% for HPT and 2.5% for HPD. The percentages are both within the 95% probability based on bootstrap realizations, implying that the overall decreasing trend of the HPT and HPD cannot be detected.

For extreme heavy precipitation, the regions with significant increasing trends over southeastern China in terms of the magnitude and frequency are larger. The percentage of stations with a significant upward trend increases to 9.3% for extreme heavy precipitation total (EHPT) and 6.3% for extreme heavy precipitation days (EHPD), both lie outside the 95% probability distribution in the histogram obtained by resampling. Only 0.8% of the stations show a significant decreasing trend. Noted that the significant trends of the intensity of the four precipitation categories show no coherent patterns, with a random distribution across China. Only the intensification of extreme heavy precipitation can be significantly detected, with a trend distribution that is slightly different from what would be expected by random chance.

The significant relationships between changes in four precipitation categories and global warming were also examined (Fig. S3 and Fig. S4). In generally, the patterns of stations showing positive (negative)

association with GMST (Fig. S3) are similar to the pattern of stations with increase (decrease) trend in Figure 3, especially in the magnitude and frequency of precipitation. In Fig. S4, we can see that the effect of global warming on the increase in the magnitude and frequency of the HP and EHP can be clearly detected. The global warming signals in decrease changes in the magnitude and frequency of LP and MP have also emerged in the observed record.

The *S* and *C* value series for the four precipitation categories are also shown to demonstrate the time at which the trend becomes significant (Figures 5 and 6). Here, we only display indices with significant trend that can be detected from 1961 to 2017, that is, a significant increase trend for heavy and extreme heavy precipitation as well as a significant decrease for light and moderate precipitation. For heavy precipitation (Figure 5), a clear separation between *S* and *C* cannot be found. However, a significant trend in extreme heavy precipitation can be detected. Taking the magnitude as an example, the percentage of stations showing a significant increase trend is nearly 3% from 1961 to 1991. This value increases to 9% from 1961 to 2017. Overall, significant trends for HP and EHP can only recently be observed. As expected, the global warming

signal of the HP and EHP trends cannot be detected (Fig. S5). Compared with HP, an effect of global warming on EHP in terms of the magnitude and frequency can be detected.

The detectability of the significant decreases in light and moderate precipitation is the most robust (Figure 6). The percentage of stations showing a significant decrease of those indices increases over time. The percentage increases from 2% during 1961 to 1991 to more than 12% and 17% during 1961 to 2017 for LPT and LPD, respectively. Significant decreasing trends in LPT and LPD can be observed close to the year around 2000. The time at which global warming affects the LPT and LPD trends is the same as the time at which the trend become significant (Fig S6), which indicates that anthropogenic global warming plays a dominate role in the detectability of significant decreases in LPT and LPD.

Overall, a significant increasing trend in the PRCPTOT, WD, and SDII can be detected across China in the period of 1961–2017, whereby the percentage of stations showing a significant trend significantly differs from what would be expected by random chance. However, only a significant increase in extreme heavy precipitation in terms of the magnitude and frequency can be robustly detected and the overall trend

only recently emerged (close to the year 2014). The detectability of the decreases in light and moderate precipitation is the most robust, with a clear difference between S and C emerging around 2000. In many previous studies, an increasing trend in extreme heavy precipitation and decreasing trend in light precipitation over China were reported (Jiang et al., 2014; Ma et al., 2015b, 2017). We have demonstrated that the observed trends of the weakest and strongest precipitation may stem from external forcing rather than from internal variability.

At the seasonal scale, the detectability in summer (JJA) is similar to that of the annual trend (Table 2). A remarkable difference is that a higher percentage of stations show a significant trend in the PRCPTOT, SDII, and WD in winter (DJF) than in summer. For example, the percentage of stations with a significant increase in WD is nearly 11.6% in winter but only 6.5% in summer. This is mainly due to the larger magnitude of warming in winter than in summer. The overall increase trend in the total precipitation can be detected in winter for all categories, except for light precipitation. However, significant decreases in the frequency of light and moderate precipitation cannot be observed in winter.

4. Conclusion

By using the daily precipitation from 603 observational stations from 1961 to 2017, we investigated the detectability of the precipitation trend for China. This was achieved using a field significance test. The trend is considered to be significant if the percentage of stations showing a significant negative or positive change is above the percentage that is expected by chance. Furthermore, the times at which the trend becomes significant and global warming has an effect were also estimated. The main findings are as follows:

- 1) An overall increasing trend in the PRCPTOT and SDII and a decreasing trend in WD were detected from 1961 to 2017 because the percentage of stations with a significant trend was greater than expected by random chance. The trend significance and effect of global warming were detected earlier for WD and SDII than for PRCPTOT.
- 2) For the four precipitation categories based on percentiles, a significant increasing trend in extreme heavy precipitation was detected recently (close to the year 2014). The detectability of the significant decreasing trend in the light precipitation is the most robust and the overall trend

become significant close to the year 2000. The time at which global warming signal in trend of precipitation characteristics emerges is the same as the time at which the trend became significant.

- 3) The detectability of the overall trend significance for the precipitation indices differs between winter and summer, especially for light and moderate precipitation. In general, more stations show a significant trend in winter than in summer.

The results presented here only seek to detect the trend significance and effect of global warming on the precipitation characteristics. In our study, we found that the overall trend significance in extreme light and extreme heavy precipitation can be detected, especially for extreme light precipitation. Future analysis show that global warming is expected to contribute to the observed trend significance. The physical mechanism behind our findings is that the increase in extreme heavy precipitation is mainly depends on the availability of atmospheric moisture, which is expected to increase as the temperature increase in response to greenhouse gases-induced warming. Furthermore, the increase in atmospheric static stability associated with anthropogenic global warming (Huang and Wen 2013) could partly account for the decreasing trend in

light precipitation (Zhao et al., 2006; Qian et al., 2009; Fu and Dan 2014). The effects of anthropogenic aerosols via aerosol radiation interaction, which may partially offset the effect of the greenhouse gases forcing, will lead to an increase in extreme light precipitation but decrease in the extreme heavy precipitation (Ma et al., 2017). However, other studies indicated that aerosols could suppress light rain through aerosol cloud interaction effect (Qian et al., 2009).

Because of the limited sample size of the observation record, the time at which the trend becomes significant obtained in this study may be a transient time rather than a stable time. For example, the percentage of stations with significant decrease trend in Fig. 2 for WD and Fig. 6 for moderate precipitation show a decreasing trend in recent years. Thus, a longer observation record is needed to improve the robustness of the result. Furthermore, the climate model simulations under future pathway scenarios could be used to verify the time at which the trend becomes significant, assuming that the models can reproduce well the precipitation characteristics over China (Jiang et al., 2015).

Acknowledgments

This work is supported by the National Key Research and Development Program of China (grant 2018YFC1507704; 2018YFC1507703; 2017YFA0603804), National Natural Science Foundation of China (41905078) and the Startup Foundation for Introducing Talent of NUIST.

Reference

- Alexander, L. V., and J. M. Arblaster, 2009: Assessing trends in observed and modelled climate extremes over Australia in relation to future projections. *Int. J. Climatol.*, 29, 417–435.
- Alexander, L.V., Zhang, X., Peterson, T.C., et al., 2006. Global observed changes in daily climate extremes of temperature and precipitation. *J. Geophys. Res.* 111 (D05109) <https://doi.org/10.1029/2005JD006290>.
- Allen, M. R., and W. J. Ingram, 2002: Constraints on future changes in climate and the hydrologic cycle. *Nature*, 419, 224–232.
- Cao, L., Zhu, Y., Tang, G., et al., 2016. Climatic warming in China according to a homogenized dataset from 2419 stations. *Int. J. Climatol.* 36, 4384-4392. <https://doi.org/10.1002/joc.4639>.
- Dai, A., 2006: Recent climatology, variability and trends in global surface humidity. *J. Climate*, 19, 3589–3606.
- Donat, M. G., Alexander, L. V., Yang, H. et al., 2013. Updated analyses of temperature and precipitation extreme indices since the beginning of the twentieth century: The HadEX2 dataset. *Journal of Geophysical Research*, 118(5), 2098-2118.
- Held, I. M., and B. J. Soden, 2006: Robust responses of the hydrological cycle to

global warming. *J. Climate*, 19, 5686–5699.

IPCC, 2013: Summary for policymakers. *Climate Change 2013: The Physical Science Basis*. T. F. Stocker et al., Eds., Cambridge University Press, 3–29.

Jiang, Z., Li, W., Xu, J., & Li, L. 2015. Extreme precipitation indices over China in CMIP5 models. Part I: Model evaluation. *Journal of Climate*, 28(21), 8603–8619.

Jiang, Z., Y. Shen, T. Ma, P. Zhai, and S. Fang, 2014: Changes of precipitation intensity spectra in different regions of mainland China during 1961–2006. *J. Meteor. Res.*, 28, 1085–1098, doi:10.1007/s13351-014-3233-1.

Huang G, Wen G H. Spatial and temporal variations of light rain events over China and the mid-high latitudes of the Northern Hemisphere. *Chin Sci Bull*, 2013, 58: 1402–1411, doi: 10.1007/s11434-012-5593-1

Karl, T. R., and R. W. Knight, 1998: Secular trends of precipitation amount, frequency, and intensity in the United States. *Bull. Amer. Meteor. Soc.*, 79, 231–241

Kiktev, D., Sexton, D. M., Alexander, L., Folland, C. K. 2003. Comparison of modeled and observed trends in indices of daily climate extremes. *Journal of Climate*, 16(22), 3560–3571.

Li, W., Jiang, Z., Zhang, X., & Li, L. 2018. On the Emergence of Anthropogenic Signal in Extreme Precipitation Change Over China. *Geophysical Research Letters*, 45(17), 9179–9185.

Liu, S. C., C. Fu, C.-J. Shiu, J.-P. Chen, and F. Wu, 2009: Temperature dependence of global precipitation extremes. *Geophys. Res. Lett.*, 36, L17702.

Lovejoy, S., Schertzer, D., and Allaire, V. 2008. The remarkable wide range spatial scaling of TRMM precipitation. *Atmospheric Research*, 90(1):10–32.

Ma, S., Zhou, T. 2015a. Observed trends in the timing of wet and dry season in China and the associated changes in frequency and duration of daily precipitation. *International Journal of Climatology*, 35(15), 4631–4641.

- Ma, S., Zhou, T., Dai, A., Han, Z. 2015b. Observed Changes in the Distributions of Daily Precipitation Frequency and Amount over China from 1960 to 2013. *Journal of Climate*, 28(17), 6960-6978.
- Ma, S., Zhou, T., Stone, D. A., Polson, D., Dai, A. et al. 2017. Detectable anthropogenic shift toward heavy precipitation over eastern China. *Journal of Climate*, 30(4), 1381-1396.
- Maskey, M. L., Puente, C. E., Sivakumar, B., and Cortis, A. 2016. Encoding daily rainfall records via adaptations of the fractal multifractal method. *Stochastic Environmental Research and Risk Assessment*, 30(7):1917–1931.
- Pendergrass, A. G. and D. L. Hartmann, 2014: The Atmospheric Energy Constraint on Global-Mean Precipitation Change. *J. Climate*, 27, 757–768.
- Qian Y, Gong D, Fan J, et al. 2009. Heavy pollution suppresses light rain in China: Observations and modeling. *Journal of Geophysical Research:Atmospheres* (1984-2012), 114(D7)
- Sun, Y., S. Solomon, A. Dai, and R. W. Portmann, 2007: How often will it rain? *J. Climate*, 20, 4801–4818, doi:10.1175/JCLI4263.1.
- Sun, Y., Zhang, X.B., Zwiers, F.W., et al., 2014. Rapid increase in the risk of extreme summer heat in Eastern China. *Nat. Clim. Change* 4, 1082 e 1085. <https://doi.org/10.1038/nclimate2410>.
- Trenberth, K. E., A. Dai, R. M. Rasmussen, and D. B. Parsons, 2003: The changing character of precipitation. *Bull. Amer. Meteor. Soc.*, 84, 1205–1218
- Wang, X. L., and Swail, V. R. 2001. Changes of extreme wave heights in Northern Hemisphere oceans and related atmospheric circulation regimes. *Journal of Climate*, 14(10), 2204-2221.
- Westra, S., Alexander, L. V., & Zwiers, F. W. 2013. Global increasing trends in annual maximum daily precipitation. *Journal of Climate*, 26(11), 3904 – 3918.

<https://doi.org/10.1175/JCLI-D-12-00502.1>

- Yin, H., Donat, M.G., Alexander, L.V., et al., 2015. Multi-dataset coMPTrison of gridded observed temperature and precipitation extremes over China. *Int. J. Climatol.* 35, 2809-2827.
- Yin, H., Sun, Y., Wan, H., et al., 2017. Detection of anthropogenic influences on the intensity of extreme temperatures in China. *Int. J. Climatol.* 37, 1229-1237. <https://doi.org/10.1002/joc.4771>.
- Yin, H, and Sun, Y. 2018. Characteristics of extreme temperature and precipitation in China in 2017 based on ETCCDI indices. *Advances in Climate Change Research*, 9(4), 218-226.
- Zhai, P., Zhang, X., Wan, H., Pan, X. 2005. Trends in total precipitation and frequency of daily precipitation extremes over China. *Journal of climate*, 18(7), 1096-1108.
- Zhang, X., H. Wan, F. W. Zwiers, G. C. Hegerl, and S. K. Min, 2013: Attributing intensification of precipitation extremes to human influence. *Geophys. Res. Lett.*, 40, 5252–5257, doi:10.1002/grl.51010.
- Zhang, X., Vincent, L. A., Hogg, W. D., & Niitsoo, A. (2000). Temperature and precipitation trends in Canada during the 20th century. *Atmosphere-ocean*, 38(3), 395-429.
- Zhang, X., Zwiers, F. W., Li, G. 2004. Monte Carlo experiments on the detection of trends in extreme values. *Journal of Climate*, 17(10), 1945-1952.
- Zhang, X., Zwiers, F. W., Hegerl, G. C., Lambert, F. H., Gillett, N. P. et al., 2007. Detection of human influence on twentieth-century precipitation trends. *Nature*, 448(7152), 461-465.
- Zhao C, Tie X, Lin Y. 2006. A possible positive feedback of reduction of precipitation and increase in aerosols over eastern central China [J]. *Geophysical Research Letters*, 33(11).

Zhao, T., and A. Dai, and J. Wang, 2012: Trends in tropospheric humidity from 1970 to 2008 over China from a homogenized radiosonde dataset. *J. Climate*, 25, 4549–4567.

Zhou, B.T., Xu, Y., Wu, J., et al., 2016. Changes in temperature and precipitation extreme indices over China: analysis of a high-resolution grid dataset. *Int. J. Climatol.* 36, 1051-1066.

Table 1 Definition of precipitation indices used in this study.

Indices	Definition
Wet days (WD)	Number of days with daily precipitation equal or greater 1 mm day ⁻¹ (day)
Total precipitation (PRCPTOT)	Total amount of precipitation from wet days (mm)
Simple precipitation intensity (SDII)	Total precipitation divided by the number of wet days (mm/day)
Light precipitation days (LPD)	Number of days with daily precipitation less than 25 th percentile of all precipitation events (day)
Light precipitation total (LPT)	Total amount of precipitation from the light precipitation days (mm)
Light precipitation intensity (LPI)	Light precipitation total divided by the light precipitation days (mm/day)
Moderate precipitation days (MPD)	Number of days with daily precipitation between 25 th and 75 th percentile of all precipitation events (day)
Moderate precipitation total (MPT)	Total amount of precipitation from the moderate precipitation days (mm)
Moderate precipitation intensity (MPI)	Light precipitation total divided by the moderate precipitation days (mm/day)
Heavy precipitation days (HPD)	Number of days with daily precipitation between the 75 th and 95 th percentile of all precipitation events (day)
Heavy precipitation total (HPT)	Total amount of precipitation from the moderate precipitation days (mm)
Heavy precipitation intensity (HPI)	Moderate precipitation total divided by the moderate precipitation days (mm/day)
Extreme heavy precipitation days (EHPD)	Number of days with daily precipitation exceeding 95 th percentile of all precipitation events (day)
Extreme heavy precipitation total (EHPT)	Total amount of precipitation from the extreme heavy precipitation days (mm)
Extreme heavy precipitation intensity (EHPI)	Extreme heavy precipitation total divided by the extreme heavy precipitation days (mm/day)

Table 2. Percentage of stations showing a significant increasing (+ve) and decreasing (-ve) trend in DJF and JJA during 1961 to 2017 for indices. Black means that the trend signal can be detected based on filed significance test.

Indicator	DJF		JJA	
	+ve	-ve	+ve	-ve
PRCPTOT	17.6%	0.3%	9%	2.5%
WD	11.6%	0.3%	6.5%	10.1%
SDII	16.7%	0.5%	10.3%	0.5%
LPT	1.7%	1.2%	2.2%	8.8%
LPD	1.2%	1.0%	2.0%	8.6%
LPI	1.5%	2.0%	3.0%	2.5%
MPT	6.3%	1.3%	3.6%	7.1%
MPD	3.8%	1.5%	3.5%	8.3%
MPI	3.0%	1.2%	3.3%	0.8%
HPT	8.5%	0.2%	6.5%	2.2%
HPD	5.3%	0.2%	5.6%	3.3%
HPI	4.3%	1.3%	6.1%	2.7%
EHPT	5.8%	0%	7.5%	0.8%
EHPD	1.6%	0%	4.6%	0%
EHPI	6.3%	0.7%	4.5%	1.7%

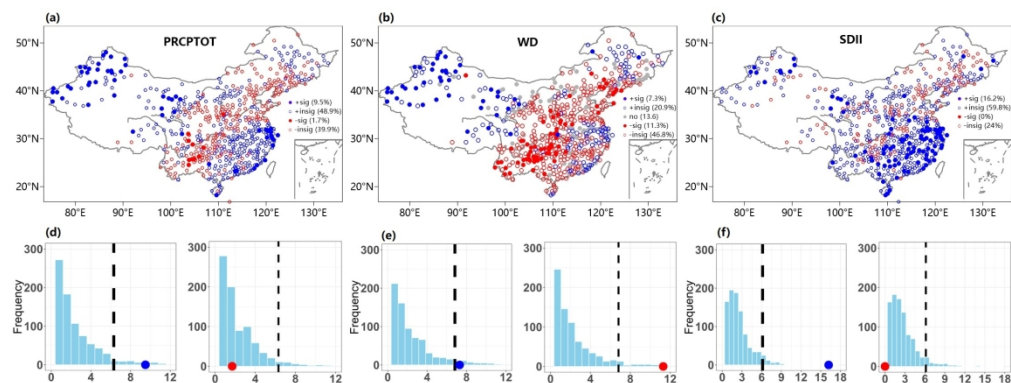


Figure 1. The pattern of trend in (a) PRCPTOT, (b) WD and (c) SDII from 1961 to 2017. The blue (red) solid circles denote significant increase (decrease) trend at the 95% confidence level. The blue (red) open circles denote insignificant increase (decrease) trend. The histograms below showing the distribution of percentage showing significant increase (left) and decrease (right) trend from 1000 bootstrap realizations for (d) PRCPTOT, (e) WD and (f) SDII, the blue (red) solid circles denote the percentage of stations showing significant increase (decrease) trend during 1961-2017, the dashed line marks the 95% probability distribution from 1000 bootstrap realizations.

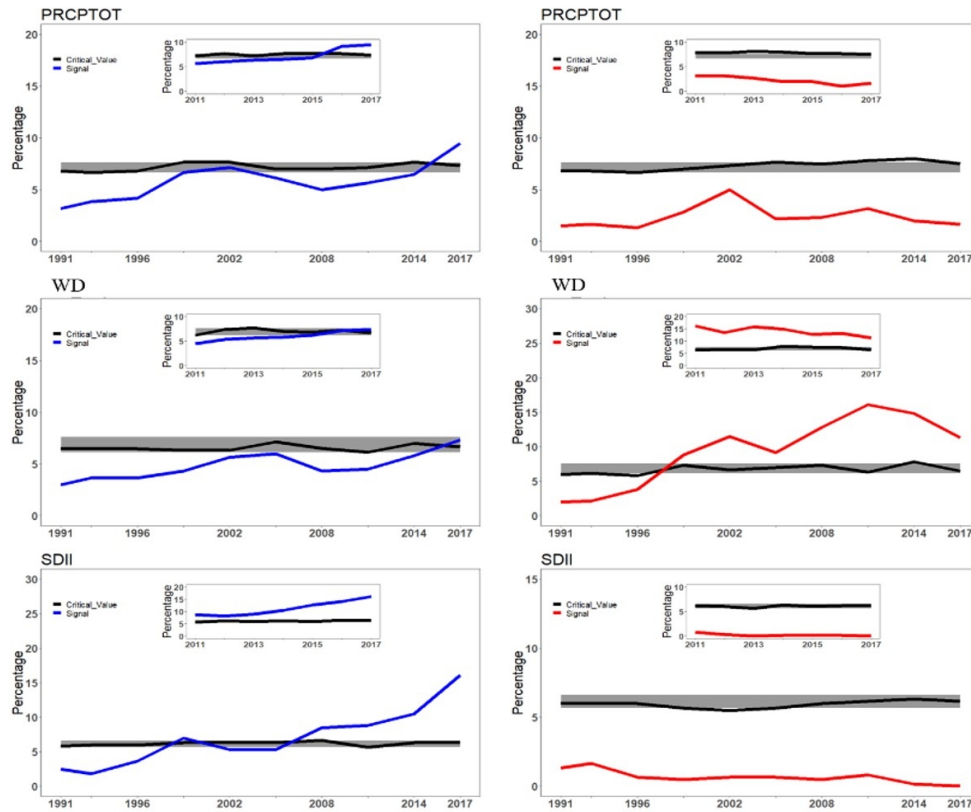


Figure 2. Blue (Red) solid line denotes the series of percentage of stations showing significant increase (decrease) trend for PRCPTOT (top row), WD (middle row) and SDII (bottom row). The gray shaded indicates the range of critical value across all period. The leftmost of x-axis in the graph shows results for 1961-1991, the calculation was then performed with an accumulative increase of three years forward until 1961 -2017, the rightmost of x-axis in the graph shows results for 1961-2017. The figure in the upper corner indicates the series from 1961-2011 with an accumulative increase of one year forward until 1961-2017.

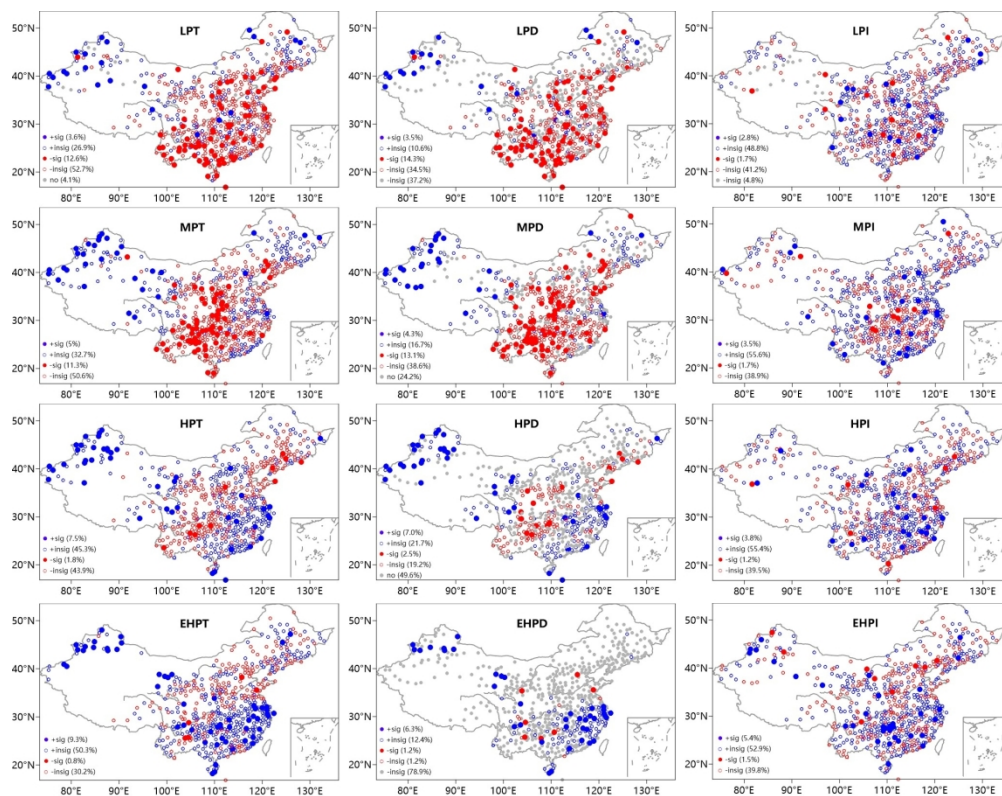


Figure 3. The trend patterns of the magnitude (left column), frequency (middle column) and intensity (right column) for light precipitation (top row), moderate precipitation (middle), heavy precipitation (bottom row) and extreme heavy precipitation (the fourth row).

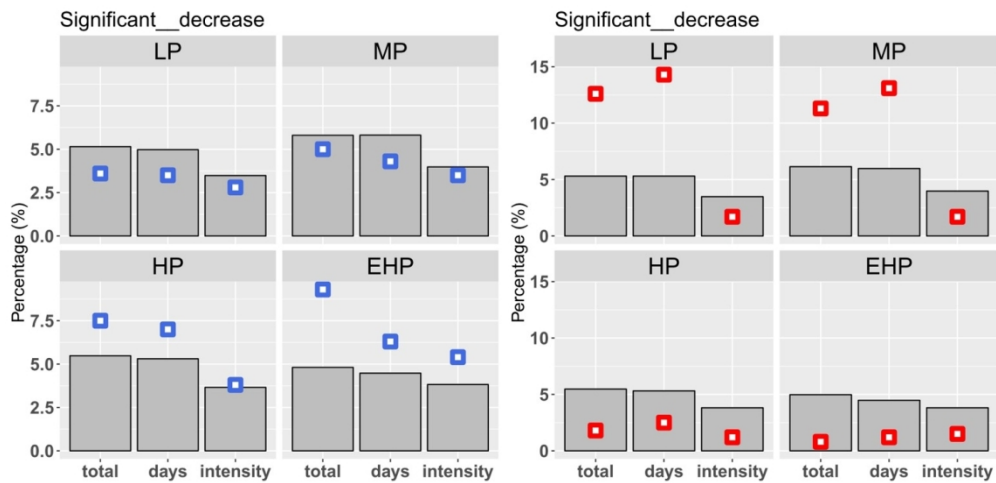


Figure 4. Left panel: Blue (Red) squares denote the percentage of stations showing a significant increasing (decreasing) trend in light precipitation (LP), moderate precipitation (MP), heavy precipitation (HP) and extreme heavy precipitation (EHP), in term of magnitude, frequency and intensity during 1961 to 2017. Gray bars denote the 95% probability in the distribution constructed with 1000 bootstrap samples.

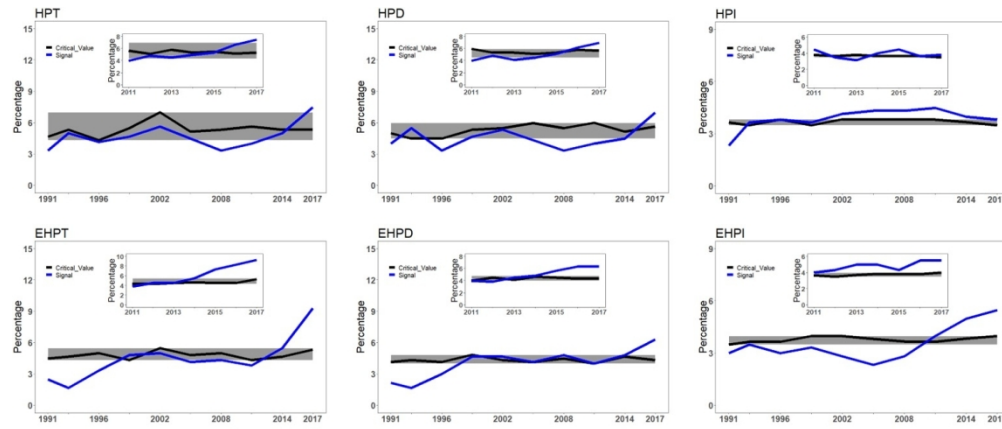


Figure 5. As for Figure 2, but for the significant increasing trend in magnitude (left column), frequency (middle column) and intensity (right column) of heavy precipitation (upper row) and extreme heavy precipitation (bottom row).

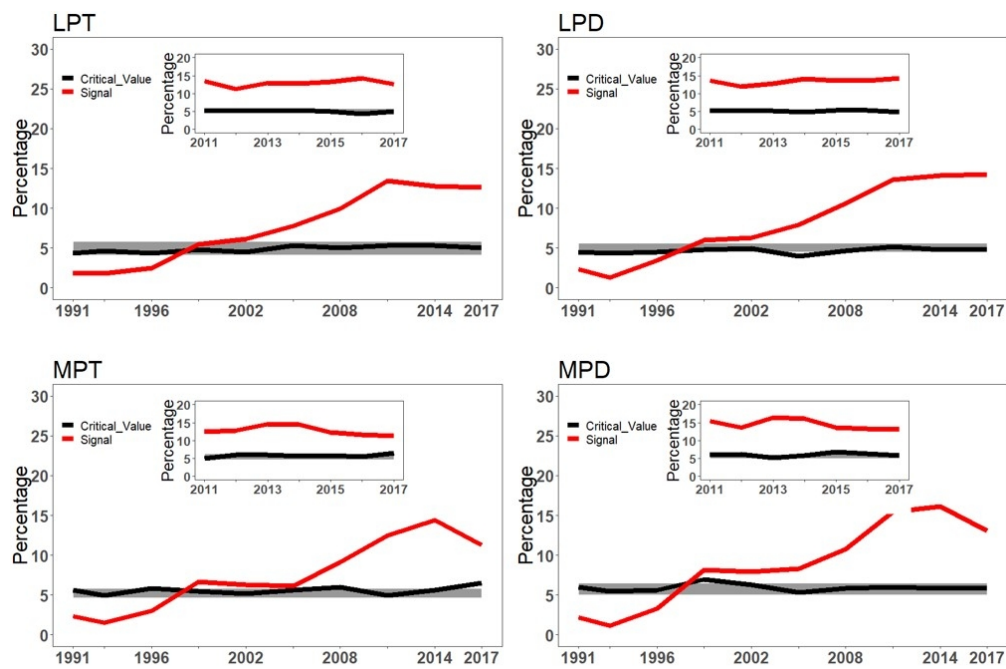


Figure 6. As for Figure 2, but for the significant decreasing trend in magnitude (left column) and frequency (right column) of little precipitation (upper row) and moderate precipitation (bottom row).